Joint User Selection and Receiver Combiner Design in Asymmetric Cell-Free Networks

Abstract

In this paper, uplink communications in cell-free networks is considered. The network channels are asymmetric in the sense that some channels are weaker than others. Access points are connected to a network controller via backhaul links. At the network controller, users' signals are decoded through the combiners that are designed by a non-convex joint sparse solver known as sparse and group sparse least absolute shrinkage and selection operator (JSGSL LASSO, shortly JSGSL). JSGSL conducts selection both at the group level (i.e., some users are selected) and at the element level (i.e., some channels in the network are selected). Numerical results highlight that the proposed JSGSL solution achieves higher selection accuracy and higher sum-rate compared to the state-of-the-art minimum mean-square error (MMSE) combiner with random selection. We also show that JSGSL can be harnessed with MMSE to reap high selection accuracy of sparse solvers and high data rate performance of MMSE combiners at the cost of increased complexity.

I. Introduction

Intelligent selection of network units, such as access points (APs) and users, can significantly improve the key performance indicators (KPIs) of a network. Some examples of KPIs can be reduced power consumption by user selection, reduced backhaul and fronthaul traffics by AP selection, and increased data rate by both user and AP selections [1].

In this paper, a highly accurate, computationally low-cost, and largely scalable algorithm is proposed to select users in the uplink communication of cell-free networks. The cell-free network channels are assumed to be asymmetric in the sense that some channel gains are significantly lower than others. E.g., some channels experience poor received signal powers or poor large-scale fading coefficients [2]. In cell-free networks, it is expected users are served by many APs rather than a few or only one [3]. For instance, users that have poor channel gains to most of the APs can be rejected to the cell-free network and disposed to other sub-networks assuming the governing network supports a heterogeneous architecture [4].

Most of the papers in cell-free literature focus on AP selection [5]–[8] rather than user selection [9]. The common selection approach in the mentioned papers is to apply combinatorial methods that impose high computational complexities, especially in cell-free networks where the numbers of users and APs are very large. Another selection approach is to use sparse solvers that design, such as the precoders, combiners, and power allocations in the network [10], [11]. The non-zero values in sparse solver solutions can directly capture the selected units in the network.

Sparse solvers can be broadly classified under two categories, solutions obtained by convex and non-convex regularization functions. In general, non-convex regularization can yield significant performance improvement over convex regularization [12]. For non-convex penalties, proximity operators are highly efficient first-order algorithms that can scale well for high dimensional problems [13], e.g., for large networks. For guaranteed convergence under mild conditions, the alternating direction method of multipliers (ADMM) is a trusted method. Hence, proximal ADMM algorithms can be favored for sparse problems that are based on non-convex regularization [14].

For asymmetric cell-free networks, sparse solvers that exploit co-occurring sparsity structures are appropriate. If channel gains of some users' are poor to most of the APs, then group sparsity-promoting solutions are good fits. On the other hand, if channel gains between some users and some APs are poor, then element sparsity-promoting solutions are preferable. In co-occurring sparsity cases, a nested, i.e., joint, solution where the output of the element proximity operator is fed to the group proximity operator outperforms the separate solution where the proximity operators are independently evaluated [13].

Transmit precoding and receive combining have been among the major pillars of multiple-input multiple-output (MIMO) wireless networks [15] to enable the next leap in future wireless technologies. Among these transceiver designs, the basic linear methods have appealing trade-offs, such as between computational complexity and data rate. In particular, the minimum mean-square error (MMSE) transceiver achieves a good data rate in a good range of signal-to-noise ratio (SNR) since MMSE considers both the interference and noise powers in its formulation. The inherent matrix inversion in MMSE formulation is a drawback for large networks, but this drawback can be diminished by applying further techniques [16]. Nonetheless, the data rate achieved by state-of-the-art MMSE transceivers can be regarded as a rudimentary benchmark.

In this paper, we propose a sparse problem solution that jointly selects the users and designs the receiver combiner in the uplink of asymmetric cell-free networks. The proposed sparse solver exploits the co-occurring sparsity at the element and group levels. The selection accuracy and data rate of the proposed solution outperform the MMSE combiner with random selection. At the expense of increased complexity, the proposed sparse solver can be harnessed with the MMSE combiner, i.e., the users are first selected by the sparse solver, and then, the MMSE combiner is designed based on the selected users. This combined solution benefits the advantages of both worlds, i.e., high user selection accuracies of the sparse solvers and high data rate performances of the MMSE combiners.

The rest of the paper is organized as follows. Section II presents the system model. Section III formulates the problem for the joint selection of users and design of receiver combiner in asymmetric cell-free networks. Section IV proposes a joint sparse and group sparse solver algorithm for the defined problem. Section IV exhibits the numerical results of the proposed solution. Finally, Section VI concludes the paper.

Notations: Throughout the paper, $(.)^T$, $(.)^H$, and $\text{tr}\{.\}$ denote the transpose, conjugate transpose, and trace operations of a matrix, respectively. $\|.\|_p$ and $\|.\|_F$ denote the ℓ_p vector and Frobenius matrix norms, respectively. a_{ij} is the entry in the i^{th} row and the j^{th} column of the matrix $\mathbf{A}$. $\mathcal{CN}(0,x)$ denotes the complex Gaussian distribution with zero mean and variance x. $E\{.\}$, $|.|$, $\lfloor.\rfloor$, and $\lceil.\rceil$ are the expectation, absolute value, flooring, and ceiling operators, respectively.

II. System Model

We consider L single-antenna access points (APs) and K single-antenna users. The received signal at AP l is given as

$$y_l = p_{\text{t}} \sum_{k=1}^{K} h_{lk} s_k + n_l, \tag{1}$$

where p_{t} is the transmit power of a user, $h_{lk} \sim \mathcal{CN}(0,1)$ is the channel between user k and AP l, $s_k \sim \mathcal{CN}(0,1)$ is the transmitted symbol from user k, and $n_l \sim \mathcal{CN}(0,\sigma^2)$ is the noise at AP l. Hence, the received signal at all APs is given as

$$\mathbf{y} = \sqrt{p_{\text{t}}}\mathbf{H}\mathbf{s} + \mathbf{n}, \tag{2}$$

where $\mathbf{y} = [y_1 \dots y_L]^T$, $\mathbf{s}$ and $\mathbf{n}$ are defined similarly, and the channel matrix between the users and APs is given as

$$\mathbf{H} = \begin{bmatrix} h_{11} & \dots & h_{1K} \\ \vdots & \ddots & \vdots \\ h_{L1} & \dots & h_{LK} \end{bmatrix}. \tag{3}$$

The cell-free network channel $\mathbf{H}$ in (3) is assumed to be asymmetric both at the element and group levels. An exemplary asymmetric cell-free network is shown in Fig. 1. The red links mark the channel gains that are weaker than the others. The channel gain matrix of such a network can supposedly be

$$\mathbf{H}_{\text{CG}} = \begin{bmatrix} \Theta_{11} & \Theta_{12} & \Theta_{13} \\ \theta_{21} & \theta_{22} & \Theta_{23} \\ \theta_{31} & \Theta_{32} & \theta_{33} \\ \theta_{41} & \Theta_{42} & \Theta_{43} \\ \theta_{51} & \Theta_{52} & \Theta_{53} \end{bmatrix}, \tag{4}$$

where Θ_{lk} and θ_{lk} denote the strong and weak channel gains, respectively, between AP l and user k. Clearly, group sparsity is imposed by user 1 while element sparsity is imposed by users 2 and 3. Thus, user 1 is to be rejected by the cell-free network while users 2 and 3 are served by only a subset of APs.

At the network controller (NC), the received signals from the users are combined as follows

$$\mathbf{V}^H\mathbf{y}, \tag{5}$$

where $\mathbf{V} = [\mathbf{v}_1 \dots \mathbf{v}_K] \in \mathbb{C}^{L\times K}$ is the combining matrix whose k^{th} column decodes the symbol of user k.

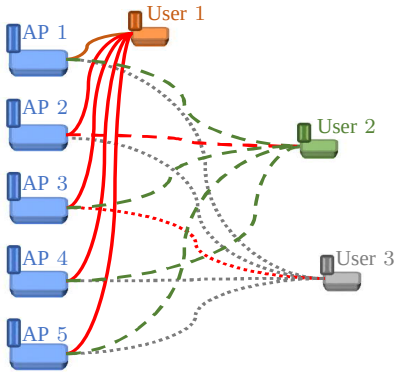

Fig. 1. Exemplary asymmetric cell-free network with 5 APs and 3 users. Red lines indicate weaker channels in the network. User 1 is to be rejected.

III. Problem Formulation

A possible combining matrix can be given as a sum mean-square error (SMSE) minimizer

$$\min_{\mathbf{V}} \varepsilon = E\{\|\mathbf{V}^H\mathbf{y} - \mathbf{s}\|_2^2\}. \tag{6}$$

The solution to (6) is known as the MMSE receiver where the vector filters $\mathbf{v}_k$ for all users contributing to the minimization of the SMSE. Sparsity-inducing terms can be included in (6) to select some users if the users' contributions to solving (6) are not significant. Hence, the total network power consumption and computational complexity can be significantly reduced.

ε in (6) can be further rewritten as

$$\begin{aligned} \varepsilon =& E\{\|\sqrt{p_{\text{t}}}\mathbf{V}^H\mathbf{H}\mathbf{s} - \mathbf{s}\|_2^2\} + E\{\|\mathbf{V}^H\mathbf{n}\|_2^2\} \\ =& \text{tr}\{\mathbf{Q}\mathbf{Q}^H\} + \sigma^2\text{tr}\{\mathbf{V}\mathbf{V}^H\}, \end{aligned} \tag{7}$$

where $\mathbf{Q} = \sqrt{p_{\text{t}}}\mathbf{V}^H\mathbf{H} - \mathbf{I}$.

Assuming maximum K_s out of K users are selected at the NC, the combining matrix can be further constrained with the inequality

$$\|\mathbf{V}\|_{2,0} \le K_s, \tag{8}$$

where $\ell_{p,q}$ norm is defined as

$$\|\mathbf{V}\|_{p,q} = \left[\sum_{k=1}^{K} (\|\mathbf{v}_k\|_p)^q\right]^{(1/q)}. \tag{9}$$

Relaxing the ℓ_0 norm in (8) with the ℓ_1 norm, the joint user selection and receiver combining problem can be given in an unconstrained form as

$$\min_{\mathbf{V}} \|\sqrt{p_{\text{t}}}\mathbf{V}^H\mathbf{H} - \mathbf{I}\|_F^2 + \sigma^2\|\mathbf{V}\|_F^2 + \beta\|\mathbf{V}\|_{2,1}, \tag{10}$$

where β is the penalty parameter.

The third summand in (10) induces sparsity at the group level, i.e., the penalty term enforces some users to be silenced thus selecting the rest of the users. To induce sparsity at the element level, i.e., some links in the network are silenced, the conventional least absolute shrinkage and selection operator (LASSO) penalty can be added to (10)

$$\begin{aligned} \min_{\mathbf{V}} \|\sqrt{p_{\text{t}}}\mathbf{V}^H\mathbf{H} - \mathbf{I}\|_F^2 + \sigma^2\|\mathbf{V}\|_F^2 + \beta\|\mathbf{V}\|_{2,1} \\ + \alpha\|\mathbf{V}\|_{1,1}, \end{aligned} \tag{11}$$

where α is the penalty parameter.

IV. Joint Sparse and Group Sparse Solution (JSGSL)

Alternating direction method of multipliers (ADMM) decomposes the problem (11) into two subproblems by introducing an auxiliary variable $\mathbf{W}$. Then the problem (11) can be rewritten as

$$\min_{\mathbf{V},\mathbf{W}} \|\sqrt{p_{\mathrm{t}}}\mathbf{V}^H\mathbf{H}-\mathbf{I}\|_F^2+\sigma^2\|\mathbf{V}\|_F^2+\rho\|\mathbf{W}-\mathbf{V}\|_F^2 + \alpha\|\mathbf{W}\|_{2,1}+\beta\|\mathbf{W}\|_{1,1}, \quad (12)$$

where ρ is the Lagrangian dual update step size.

For fixed $\mathbf{W}$, the first subproblem is given as

$$\min_{\mathbf{V}} \|\sqrt{p_{\mathrm{t}}}\mathbf{V}^H\mathbf{H}-\mathbf{I}\|_F^2+\sigma^2\|\mathbf{V}\|_F^2+\rho\|\mathbf{W}-\mathbf{V}\|_F^2. \quad (13)$$

The above subproblem is quadratic in $\mathbf{V}$ and has a simple closed-form solution given as

$$\mathbf{AV}=\sqrt{p_{\mathrm{t}}}\mathbf{H}+\rho\mathbf{W}, \quad (14)$$

where $\mathbf{A}=p_{\mathrm{t}}\mathbf{H}\mathbf{H}^H+\left(\sigma^2+\rho\right)\mathbf{I}$.

For fixed $\mathbf{V}$, the second subproblem is given as

$$\min_{\mathbf{W}} \rho\|\mathbf{W}-\mathbf{V}\|_F^2+\alpha\|\mathbf{W}\|_{2,1}+\beta\|\mathbf{W}\|_{1,1}. \quad (15)$$

The sparse [17] and group sparse [18] LASSO solutions can be jointly utilized as a convex solution for (15) [19]. However, non-convex solutions which utilize non-convex penalty functions including $\ell_p, p<1$ pseudo-norm are known to yield improved results compared to convex solutions [14]. The non-convex solution can be computed in a nested fashion [13]. That is, the inner shrinkage operator maps the element-level sparsity on the last summand in (15). Then the output is fed into the outer shrinkage operator that maps the group-level sparsity on the second summand in (15). Assume G is the group size of the solution in (15). Hence, $\|\mathbf{W}\|_{2,1}$ in (15) can be rewritten as

$$\sum_{k=1}^{K}\sum_{g=1}^{G}\|\mathbf{w}_k^g\|_2, \quad (16)$$

where $\mathbf{w}_k^g$ is the g^{th} row group of $\mathbf{w}_k$, and $\mathbf{w}_k$ is the k^{th} column of $\mathbf{W}$, i.e.,

$$\mathbf{W}=\begin{bmatrix}\mathbf{w}_1^1 & \cdots & \mathbf{w}_K^1\\ \vdots & \ddots & \vdots\\ \mathbf{w}_1^g & \cdots & \mathbf{w}_K^g\end{bmatrix}.$$

The group sparse solutions can be categorized under two classes [20]: non-overlapping and overlapping group sparse solutions. In the former case, the variables are decoupled. Since the optimization problem is simpler in this case, we opt for this option. Then the element-level and group-level sparsity on the third and second summands in (15) are achieved by the following shrinkage mappings

$$S_p(\mathbf{w}_k,\alpha/\rho)_i=\frac{w_{ki}}{|w_{ki}|}\max\left\{0,|w_{ki}|-(\alpha/\rho)^{2-p}|w_{ki}|^{p-1}\right\} \text{ and}$$
$$S_q(\mathbf{w}_k,\beta/\rho)=\frac{\mathbf{w}_k}{\|\mathbf{w}_k\|_2}\max\left\{0,\|\mathbf{w}_k\|_2-(\beta/\rho)^{2-q}\|\mathbf{w}_k\|_2^{q-1}\right\}, \quad (17)$$

respectively, where w_{ki} is the i^{th} element of $\mathbf{w}_k$. Finally, the nested shrinkage mapping for joint sparse and group sparse solution is given as

$$\mathbf{w}_k=S_q(S_p(\mathbf{v}_k,\alpha/\rho),\beta/\rho). \quad (18)$$

Introducing the dual variable $\mathbf{\Lambda}$ to enforce the equality of $\mathbf{W}$ and $\mathbf{V}$, the ADMM solution for (11) is given in Algorithm 1. In Algorithm 1, $0\le\gamma\le 1$, is the sparsity rate of the network, which is inversely related with the number of selected users K_s, $K_s=K-\lfloor\gamma K\rfloor$. For improved performance, the penalty parameters α and β, step size ρ, the non-convexity parameters p and q, and the group size parameter G are searched over a search set of length T as seen in Algorithm 1. The values of these parameters are detailed in Section V. The optimal parameters are determined based on the sum-rate metric of the network which is given as

$$R=\sum_{k=1}^{K}R_k, \quad (19)$$

where the rate of user k is given as

$$R_k=\log_2\left(1+\gamma_k\right),$$

where

$$\gamma_k=\frac{p_{\mathrm{t}}\left|\sum_{l=1}^{L}v_{lk}^*h_{lk}\right|^2}{p_{\mathrm{t}}\sum_{\substack{j=1\\ j\neq k}}^{K}\left|\sum_{l=1}^{L}v_{lj}^*h_{lj}\right|^2+\sigma^2}$$

is the signal-to-interference-plus-noise ratio (SINR) of user k.

Hence, the optimal solution $\mathbf{V}^\star$ is obtained by the optimal parameters indexed by $t^\star$, i.e., $\mathbf{V}^\star=\mathbf{V}_t^\star$.

In Algorithm 1, two loops are iterated by the loop control variables m_Λ and Δ_W for the sake of fast executions of the

Algorithm 1 Proposed Joint Sparse and Group Sparse Solution via ADMM for (11).

1) Initialize the auxiliary and Lagrangian variables, $\mathbf{W}=\mathbf{0},\mathbf{\Lambda}=\mathbf{0}$. 2) If the algorithm parameters such as α, β, and ρ are not fixed, determine their ranges to be screened.

$R=0, t=1$
while $t\le T$ **do**
  $R'=R, \mathbf{\Lambda}'=\mathbf{\Lambda}, \mathbf{W}'=\mathbf{W}$
  $iter_o=1, iter_i=1$
  while $m_\Lambda>\epsilon$ & $iter_o\le iter_{o,max}$ **do**
    while $\Delta_W>\epsilon$ & $iter_i\le iter_{i,max}$ **do**
      Solve $\mathbf{V}$ from (14)
      Evaluate $\mathbf{w}_k,\forall k$ from (18)
      Evaluate $\Delta_W=\|\mathbf{W}'-\mathbf{W}\|_{1,1}/LK$
      $iter_i=iter_i+1$
    end while
    Update $\mathbf{\Lambda}=\mathbf{\Lambda}+\rho(\mathbf{V}-\mathbf{W})$
    Evaluate $m_\Lambda=\|\mathbf{\Lambda}\|_{1,1}/LK$
    $iter_o=iter_o+1$
  end while
  Reject $\lfloor\gamma K\rfloor$ users with the highest ℓ_2 norms, i.e., $\|\mathbf{v}_k\|_2>\|\mathbf{v}_j\|_2$
  Evaluate R
    if $R>R'$ **then** assign $t^\star=t$ **end**
  $t=t+1$
end while
Assign $\mathbf{V}^\star=\mathbf{V}_{t^\star}$

Table I: SUM-RATES, SUM-RATE DIFFERENCES, AND ACCURACIES FOR VARYING p_t (dBm), γ and fixed $L = 128, K = 32$.

	R (b/s/Hz)			ΔR (%)		Accuracy (%)	
(p_t, γ, K_s)	MMSE-R	JSGSL	MMSE-J	JSGSL & MMSE-R	MMSE-J & MMSE-R	MMSE-R	JSGSL
(5, 0.3, 23)	101	110	113	9	12	70	95
(5, 0.5, 16)	67	76	80	13	19	51	90
(5, 0.7, 10)	41	48	52	19	27	32	85
(20, 0.3, 23)	214	222	226	4	6	72	96
(20, 0.5, 16)	144	154	159	7	10	47	90
(20, 0.7, 10)	89	97	101	8	13	33	85

algorithm compared to solely setting a fixed number of outer and inner loops. It is observed that both loops iterate only a few times for the optimal and near-optimal variables in the search set. On the other hand, for the other variables in the search set, the number of iterations can hit the maximum limits $iter_{o,max}$ and $iter_{i,max}$ for the outer and inner loops, respectively.

For the interested reader, the complete codes of the proposed algorithms are shared online [21].

A. Weighted JSGSL

At the cost of small computational increase, weighted JSGSL (WJSGSL) is proposed in this section.

WJSGSL is derived from the weighted SMSE (WSMSE) minimization problem that can be given as $\varepsilon_w = \sum_{k=1}^{K} \psi_k \varepsilon_k - \log \psi_k$, where ψ_k and ε_k are the weighting coefficient and mean-square error (MSE) of user k, respectively. Then the WSMSE minimization problem is given as

$$\min_{\mathbf{v}_k, \psi_k, \forall k} \sum_{k=1}^{K} \psi_k \varepsilon_k - \log \psi_k + \beta \|\mathbf{v}_k\|_2 + \alpha \|\mathbf{v}_k\|_1 \tag{20}$$

The sum-rate maximization problem is given as

$$\max_{\mathbf{v}_k, \forall k} \sum_{k=1}^{K} R_k - \beta \|\mathbf{v}_k\|_2 - \alpha \|\mathbf{v}_k\|_1. \tag{21}$$

The equivalence of problems (20) and (21) [22], [23] is achieved at the following solutions

$$\mathbf{v}_k = \mathbf{B}_k^{-1} \left(\sqrt{p_t} \psi_k \mathbf{h}_k + \rho \mathbf{w}_k \right), \tag{22}$$

where $\mathbf{B}_k = \psi_k p_t \sum_{i=1}^{K} \mathbf{h}_i \mathbf{h}_i^H + (\sigma^2 \psi_k + \rho)\mathbf{I}$, and.

$$\psi_k = \left[\mathbf{I} - p_t \mathbf{H}^H \mathbf{A}^{-1} \mathbf{H} \right]_{k,k}^{-1}, \tag{23}$$

where $[.]_{k,k}$ denotes the k^{th} diagonal element of a matrix.

V. Numerical Results

In this section, the numerical results demonstrate the effectiveness of the proposed JSGSL solution to jointly select the users and design the receiver combiner in the asymmetric cell-free network. JSGSL achieves a higher user selection accuracy and sum-rate than achieved by MMSE with random selection (MMSE-R). Hence, MMSE-R is considered as a lower bound in numerical benchmarks. To further improve the sum-rate achieved by JSGSL at the cost of increased complexity, we also propose successive implementation of JSGSL to select the users, and then implementation of MMSE for the selected users (JSGSL-MMSE, shortly MMSE-J). This successive implementation combines the high user selection accuracy of JSGSL and the high sum-rate performance of MMSE yielding higher sum-rate results over MMSE-R and MMSE-J.

For all simulations, a laptop computer with Intel i7-7700 CPU, 2.80 GHz, 16 GB RAM, with 2 cores and 4 logical processors is used.

We assume log-normal shadowing, distance, penetration loss, and power efficiency vary with a uniform distribution between 7-9 dB, 35-50 m, 20-30 dB, and 5-10%, respectively. We assume the channel center frequency, bandwidth, noise figure, and transmit power are 2 GHz, 10 MHz, 5 dB, and 5 or 20 dBm, respectively.

The number of channel realizations is set to 20. The elements in channel $\mathbf{H}$ are drawn i.i.d. with $h_{lk} \sim \mathcal{CN}(0, 1)$ distribution. To evaluate the user selection accuracy of the proposed JSGSL solution, the channels in the network are later deliberately weakened in a way to represent asymmetric cell-free networks as detailed in Section II. The weakened channel matrix is denoted by $\mathbf{H}'$. The channels of the users with many weakened channels, i.e., the users to be rejected, are denoted by $\mathbf{h}'_j$, e.g., user 1 in (4). We vary the sparsity rate of the network γ at 0.3, 0.5, and 0.7. The higher the γ means the more rejected users in the network. We also weaken only a few channels of the users with many strong channels, i.e., the users to be selected. We set this ratio to 0.1, i.e., $\lfloor 0.1L \rfloor$ links of user k, with channel $\mathbf{h}'_k$, are weakened, e.g., users 2 and 3 in (4), where $\lceil 0.1L \rceil$ is applied for convenience.

To avoid trivial user selection solutions such as based on ℓ_2 norms of the channels, i.e., reject user j if $\|\mathbf{h}'_j\|_2 < \|\mathbf{h}'_k\|_2$, we add artificial channel spikes at a few locations in $\mathbf{h}'_j$, e.g., $h'_{lj} = 5h_{lj}, l \in \{1, 10, 20, 30\}$ if $L \geq 30$. Another trivial selection is to count the number of weakened channels of the users below a threshold τ, i.e., reject user j if $|h'_{lj}| < \tau, l \in \{1, \ldots, L_j\}$, $|h'_{lk}| < \tau, l \in \{1, \ldots, L_k\}$, and $L_j > L_k$. To avoid this trivial solution, we vary the weakened channel values of the users $\mathbf{h}'_j$ around the low-end power profile of the stronger users' $\mathbf{h}_k, k \neq j$ channel values. For the sake of exposition, consider a figurative channel gain matrix as follows for the exemplary asymmetric cell-free network presented in Fig. 1,

$$\mathbf{H}_{\text{CG}} = \begin{bmatrix} 10 & 5 & 5 \\ 2 & 1 & 4 \\ 2 & 3 & 1 \\ 1 & 2 & 2 \\ 1 & 1 & 1 \end{bmatrix}. \tag{24}$$

Clearly, the sparse solver is expected to select users 2 and 3. However, the ℓ_2 norm concludes users 1 and 3 to be selected, e.g., column sums of $\mathbf{H}_{\text{CG}} = [16\ 12\ 13]$. Next, we try counting the number of weak channel gains. Assuming a threshold $\tau < 2$, all users count to 2. Hence, a decision cannot be reached. Next, assuming a threshold $\tau < 3$, users $1, 2$, and 3 count to $4, 3$, and 3, respectively. Hence, a correct decision is reached. However, in cell-free networks where the number of APs and users are very large and channel gains are real numbers, such brute-force decision based on a thresholding mechanism is not feasible.

Finally, for each channel instance, we screen a small set of parameters for G in (16), and α, β, ρ, p, and q in (17). We also notice that mollification can help to improve the performance, e.g., by replacing $|w_{ki}|^{p-1}$ and $\|\mathbf{w}_k\|_2^{q-1}$ in (17) by $|w_{ki} + p_\epsilon|^{p-1}$ and $\|\mathbf{w}_k + q_\epsilon\|_2^{q-1}$, respectively. Three sets are used for screening, $s_1 = \{10^{-3}, 10^{-2}\}$, $s_2 = \{-2, 0\}$ and $s_3 = \{2, 4\}$. The optimal parameters are searched in the union of these sets $\alpha/\rho, \beta/\rho, p_\epsilon, q_\epsilon \in s_1$, $p, q \in s_2$, and $G \in s_3$. Hence, size of the search set T is 128. As mentioned in Section IV, loop control variables enable fast executions of the proposed algorithms. Thus, even with the screening of parameters, the simulation durations range from only 2 to 15 minutes for the smallest ($L = 128, K = 32, \gamma = 0.7$) and largest ($L = 256, K = 64, \gamma = 0.3$) network sizes, respectively. These simulation durations include simultaneous executions of JSGSL, MMSE-R, and MMSE-J solutions. For all simulations, $\epsilon, iter_{i,max}$ and $iter_{o,max}$ are set to $10^{-4}, 20$ and 200, respectively.

In Table I, the numerical results for the network with $L = 128$ and $K = 32$ for 5 and 20 dBm transmit power per user are presented. The sum-rate difference percentage is evaluated by subtracting the small value from the large value and then dividing by the small value, e.g., $\Delta R_{\text{JSGSL\&MMSE-R}} = (R_{\text{JSGSL}} - R_{\text{MMSE-R}})/R_{\text{MMSE-R}} * 100$. ΔR is sub-indexed so that the larger value is written first. As seen in the results, at a low signal-to-noise ratio (SNR), accurate selection of users is more critical to achieving high sum-rate results, i.e., ΔR at low SNR is higher than that of at high SNR. Although the selection accuracy of MMSE-R is significantly worse than JSGSL, its sum-rate is still close to JSGSL. The main reason is the addition of spikes in weak users' channels as mentioned earlier. Hence, if MMSE-R chooses a weak user instead of rejecting it, the rate punishment for the wrong decision is milder due to the artificial spikes in the weak users' channels.

In Table II, the numerical results for the network with $L = 128, 256$ and $K = 32, 64$ for 20 dBm transmit power per user are presented. When L is fixed and γ is increased, selection becomes a more challenging task since a few out of many users need to be selected. Thus, for both JSGSL and MMSE-R, the selection accuracies drop as γ increases. However, the drop is significantly milder for JSGSL than the random selection. When K is fixed and L is increased, the selection accuracy of JSGSL increases since the number of observations for a sparse solution increases.

In Table III, we investigate the benefit of JSGSL considering the trade-off between sum-rate and power consumption in the network. Therefore, we compare the proposed advanced selection algorithm MMSE-J with the no selection algorithm MMSE-NS. In other words, the MMSE-NS algorithm assumes all users participate in the uplink communications and MMSE receiver combiner is applied. Since the accuracy of the proposed algorithm is already demonstrated in earlier results, spikes in weak users' channels are not added for the results obtained in Table III. Hence, the true sum-rate gap between MMSE-J and MMSE-NS are observed. The sum-rate gaps in Table III are always evaluated by $\Delta R'_{\text{MMSE-NS\&J}} = (R_{\text{MMSE-NS}} - R_{\text{MMSE-J}})/R_{\text{MMSE-J}} * 100$ although sometimes the sum-rate of MMSE-J is higher than MMSE-NS. Hence, negative values are obtained in certain cases. The positive values next to the negative values are evaluated by the sum-rate gap definition given earlier, i.e., the sum-rate difference percentage ΔR is evaluated by subtracting the small value from the large value and then dividing by the small value.

As seen in Table III, at high SNR, when $\Delta R' \geq 0$, the sum-rate gap is smaller because MMSE-NS benefits from any user in the network even including the users with poor connections at high SNR regime. But at low SNR, the users with poor connections do not make much of a difference to contribute to the sum-rate. At low SNR and for $L = 24, 32$, MMSE-J performs better since the network is interference limited in the MMSE-NS case due to insufficient L value compared to K_s. This effect is still observed at high SNR for $L = 24$. When the network is not interference limited, MMSE-NS is considered as an upper bound in numerical benchmarks. The results clearly demonstrate the beneficial trade-off of the proposed algorithm. In the worst scenario, $\Delta R' = 39\%$ but this is achieved by MMSE-NS at the cost of significantly high number of users, i.e., the increase is $(64 - 20)/20 * 100 = 220\%$. In the best scenario, $\Delta R' = 3\%$ and with a good trade-off since the number of users increases by $(32 - 23)/23 * 100 = 39\%$. 3% loss vs. 39% gain is a remarkably advantageous trade-off especially if energy efficiency of the cell-free network is a concern.

As noted earlier, in Tables I and II, the sum-rate gaps between MMSE-R and JSGSL is milder due to the added channel spikes. To demonstrate the true sum-rate gap between MMSE-J and MMSE-R, the numerical results without added channel spikes are presented in Table IV. The conclusions reached for Table I are also valid for Table IV with only difference that the sum-rate gaps are now more remarkable as expected.

Finally, in Table V, the improved sum-rate results of WJSGSL over JSGSL are presented.

VI. Conclusion

In this paper, we present an effective user selection algorithm based on a sparse and group sparse solver solution

Table II: SUM-RATES, SUM-RATE DIFFERENCES, AND ACCURACIES FOR VARYING L, K, γ and fixed $p_t = 20$ dBm.

	R (b/s/Hz)			ΔR (%)		Accuracy (%)	
(L, K, γ, K_s)	MMSE-R	JSGSL	MMSE-J	JSGSL & MMSE-R	MMSE-J & MMSE-R	MMSE-R	JSGSL
(128, 32, 0.3, 23)	214	222	226	4	6	72	96
(128, 32, 0.5, 16)	144	154	159	7	10	47	90
(128, 32, 0.7, 10)	89	97	101	8	13	33	85
(128, 64, 0.3, 45)	405	408	426	1	5	71	94
(128, 64, 0.5, 32)	280	291	311	4	11	51	91
(128, 64, 0.7, 20)	175	182	198	4	13	33	87
(256, 32, 0.3, 23)	242	249	251	3	4	74	98
(256, 32, 0.5, 16)	163	173	175	6	7	51	97
(256, 32, 0.7, 10)	100	110	111	10	11	30	94
(256, 64, 0.3, 45)	462	479	485	4	5	69	97
(256, 64, 0.5, 32)	321	342	349	6	9	50	95
(256, 64, 0.7, 20)	200	213	220	7	10	31	93

Table III: SUM-RATES AND SUM-RATE DIFFERENCES WITHOUT CHANNEL SPIKES FOR VARYING $p_t, L, K,$ and γ.

	R (b/s/Hz)		ΔR (%)		R (b/s/Hz)		ΔR (%)
(p_t, L, K, γ, K_s)	MMSE-J	MMSE-NS	MMSE-J&NS	p_t	MMSE-J	MMSE-NS	MMSE-J&NS
(5, 24, 32, 0.3, 23)	36	35	1	20	109	94	15
(5, 24, 32, 0.7, 10)	22	20	8	20	65	70	-7
(5, **24**, 64, 0.3, **45**)	37	32	14	20	79	42	**90**
(5, 24, 64, **0.7**, 20)	16	26	-61	20	43	87	**-100**
(5, 32, 32, 0.3, 23)	49	47	4	20	141	140	0
(5, 32, 32, 0.7, 10)	27	26	3	20	74	81	-10
(5, **32**, 64, 0.3, **45**)	54	51	7	20	147	71	**108**
(5, 32, 64, 0.7, 20)	44	39	11	20	123	129	-5
(5, 64, 32, 0.3, 23)	83	84	0	20	194	200	-4
(5, 64, 32, 0.7, 10)	39	40	-2	20	87	106	-22
(5, 64, 64, 0.3, 45)	130	126	3	20	327	327	0
(5, 64, 64, 0.7, 20)	74	74	-1	20	170	194	-14
(5, 128, 32, 0.3, 23)	111	112	-1	20	224	238	-6
(5, 128, 32, **0.7**, 10)	50	53	-6	20	100	138	-39
(5, 128, 64, 0.3, 45)	204	205	-1	20	423	443	-5
(5, 128, 64, **0.7**, 20)	97	102	-5	20	196	258	-32

Table IV: SUM-RATES AND SUM-RATE DIFFERENCES WITHOUT CHANNEL SPIKES FOR VARYING $p_t, L, K,$ and γ.

	R (b/s/Hz)		ΔR (%)		R (b/s/Hz)		ΔR (%)
(p_t, L, K, γ, K_s)	MMSE-J	MMSE-R	MMSE-J&R	p_t	MMSE-J	MMSE-R	MMSE-J&R
(5, 128, 32, 0.3, 23)	111	81	37	20	224	174	29
(5, 128, 32, 0.7, 10)	50	17	204	20	100	43	132
(5, 128, 64, 0.3, 45)	204	151	35	20	423	321	32
(5, 128, 64, 0.7, 20)	97	39	148	20	196	93	110

Table V: SUM-RATES AND SUM-RATE DIFFERENCES WITHOUT CHANNEL SPIKES FOR VARYING K, γ and fixed $p_t = 5$ dBm, $L = 128$.

	R (b/s/Hz)		ΔR (%)
(K, γ, K_s)	JSGSL	WJSGSL	WJSGSL& JSGSL
(64, 0.3, 45)	189	194	3
(64, 0.5, 32)	137	142	4
(128, 0.3, 90)	234	268	15
(128, 0.5, 64)	190	212	12

JSGSL that achieves higher selection accuracy and sum-rate than the state-of-the-art MMSE combiner with random selection (MMSE-R). At the increased computational complexity, JSGSL can be exercised for only user selection followed by the MMSE design as a combiner (MMSE-J). The latter solution fuses both accurate selection and high sum-rate strengths of JSGSL and MMSE, respectively, that yields a higher sum-rate than the sole implementations of MMSE-R and JSGSL. Furthermore, the proposed solution is demonstrated to provide a significant advantage in the trade-off since a low sum-rate loss is observed with a significantly less number of selected users.

The proposed JSGSL solution can be straightforwardly extended in an ad-hoc manner for joint user, AP selection, and receive combiner design. However, the rigid extension of JSGL to jointly consider group sparse columns (for AP selection) as well as group sparse rows (for user selection, as proposed in this paper) is not trivial and can be a promising theoretical future research direction.

REFERENCES

[1] A. L. Imoize, H. I. Obakhena, F. I. Anyasi, and S. N. Sur, "A review of energy efficiency and power control schemes in ultra-dense cell-free massive MIMO systems for sustainable 6G wireless communication," *Sustainability*, vol. 14, no. 17, 2022. [Online]. Available: https://www.mdpi.com/2071-1050/14/17/11100

[2] E. Björnson and L. Sanguinetti, "Making cell-free massive MIMO competitive with MMSE processing and centralized implementation," *IEEE Trans. Wireless Commun.*, vol. 19, no. 1, pp. 77–90, Jan. 2020.

[3] J. Zhang, E. Björnson, M. Matthaiou, D. W. K. Ng, H. Yang, and D. J. Love, "Prospective multiple antenna technologies for beyond 5G," *IEEE J. Sel. Areas Commun.*, vol. 38, no. 8, pp. 1637–1660, Jun. 2020.

[4] M. Sanjabi, M. Razaviyayn, and Z. Q. Luo, "Optimal joint base station assignment and beamforming for heterogeneous networks," *IEEE Trans. Signal Process.*, vol. 62, no. 8, pp. 1950–1961, Jan. 2014.

[5] H. Q. Ngo, L. N. Tran, T. Q. Duong, M. Matthaiou, and E. G. Larsson, "On the total energy efficiency of cell-free massive MIMO," *IEEE Trans. Green Commun. Netw.*, vol. 2, no. 1, pp. 25–39, Mar. 2018.

[6] J. Zhang, S. Chen, Y. Lin, J. Zheng, B. Ai, and L. Hanzo, "Cell-free massive MIMO: a new next-generation paradigm," *IEEE Access*, vol. 7, pp. 99 878–99 888, Jul. 2019.

[7] G. Femenias, N. Lassoued, and F. Riera-Palou, "Access point switch ON/OFF strategies for green cell-free massive MIMO networking," *IEEE Access*, vol. 8, pp. 21 788–21 803, Jan. 2020.

[8] S. Chen, J. Zhang, E. Björnson, O. T. Demir, and B. Ai, "Sparse large-scale fading decoding in cell-free massive MIMO systems," in *Proc. IEEE Signal Process. Adv. in Wireless Commun.*, July 04-06, 2022, pp. 1–5.

[9] G. Femenias and F. Riera-Palou, "Cell-free millimeter-wave massive MIMO systems with limited fronthaul capacity," *IEEE Access*, vol. 7, pp. 44 596–44 612, Mar. 2019.

[10] T. X. Vu, S. Chatzinotas, S. Shahbazpanahi, and B. Ottersten, "Joint power allocation and access point selection for cell-free massive MIMO," in *Proc. IEEE Int. Conf. on Commun.*, June 07-11, 2020, pp. 1–7.

[11] J. Lin, Q. Li, C. Jiang, and H. Shao, "Joint multirelay selection, power allocation, and beamformer design for multiuser decode-and-forward relay networks," *IEEE Trans. Veh. Technol.*, vol. 65, no. 7, pp. 5073–5087, Jul. 2016.

[12] F. Wen, L. Chu, P. Liu, and R. C. Qiu, "A survey on nonconvex regularization-based sparse and low-rank recovery in signal processing, statistics, and machine learning," *IEEE Access*, vol. 6, pp. 69 883–69 906, Nov. 2018.

[13] S. Beygi, U. Mitra, and E. G. Ström, "Nested sparse approximation: structured estimation of V2V channels using geometry-based stochastic channel model," *IEEE Trans. Signal Process.*, vol. 63, no. 18, pp. 4940–4955, Sep. 2015.

[14] R. Chartrand and B. Wohlberg, "A nonconvex ADMM algorithm for group sparsity with sparse groups," in *Proc. IEEE Int. Conf. on Acoustics, Speech, and Signal Process.*, May 26-31, 2013, pp. 6009–6013.

[15] M. A. Albreem, A. H. Habbash, A. M. Abu-Hudrouss, and S. S. Ikki, "Overview of precoding techniques for massive MIMO," *IEEE Access*, vol. 9, pp. 60 764–60 801, Apr. 2021.

[16] N. Fatema, G. Hua, Y. Xiang, D. Peng, and I. Natgunanathan, "Massive MIMO linear precoding: a survey," *IEEE Systems Journal*, vol. 12, no. 4, pp. 3920–3931, Dec. 2018.

[17] R. Tibshirani, "Regression shrinkage and selection via the LASSO," *Journal of the Royal Statistical Society: Series B (Methodological)*, 1996.

[18] M. Yuan and Y. Lin, "Model selection and estimation in regression with grouped variables," *Journal of the Royal Statistical Society. Series B: Statistical Methodology*, 2006.

[19] J. Friedman, T. Hastie, and R. Tibshirani, "A note on the group LASSO and a sparse group LASSO," Department of Statistics, Stanford University, Tech. Rep., 2010.

[20] P. Y. Chen and I. W. Selesnick, "Group-sparse signal denoising: non-convex regularization, convex optimization," *IEEE Trans. Signal Process.*, vol. 62, no. 13, pp. 3464–3478, Jul. 2014.

[21] C. M. Yetis, "GitHub repository. Accessed: January 17, 2023." [Online]. Available: https://github.com/DrCMY/JointDesigninAsymmetricCellFreeNetworks.

[22] Q. Shi, M. Razaviyayn, Z. Q. Luo, and C. He, "An iteratively weighted MMSE approach to distributed sum-utility maximization for a MIMO interfering broadcast channel," *IEEE Trans. Signal Process.*, vol. 59, no. 9, pp. 4331–4340, Sep. 2011.

[23] M. Hong, R. Sun, H. Baligh, and Z. Q. Luo, "Joint base station clustering and beamformer design for partial coordinated transmission in heterogeneous networks," *IEEE J. Sel. Areas Commun.*, vol. 31, no. 2, 2013.